

Phase Coupling in a Cerebro-Cerebellar Network at 8–13 Hz during Reading

Jan Kujala¹, Kristen Pammer^{1,2}, Piers Cornelissen³, Alard Roebroeck⁴, Elia Formisano⁴ and Riitta Salmelin¹

¹Brain Research Unit, Low Temperature Laboratory, Helsinki University of Technology, FIN-02015 TKK, Finland, ²School of Psychology, Australian National University, Canberra ACT 0200, Australia, ³School of Biology and Psychology, University of Newcastle, Newcastle upon Tyne NE2 4HH, UK and ⁴Department of Cognitive Neuroscience, Faculty of Psychology, University of Maastricht, 6200 MD Maastricht, The Netherlands

Words forming a continuous story were presented to 9 subjects at frequencies ranging from 5 to 30 Hz, determined individually to render comprehension easy, effortful, or practically impossible. We identified a left-hemisphere neural network sensitive to reading performance directly from the time courses of activation in the brain, derived from magnetoencephalography data. Regardless of the stimulus rate, communication within the long-range neural network occurred at a frequency of 8–13 Hz. Our coherence-based detection of interconnected nodes reproduced several brain regions that have been previously reported as active in reading tasks, based on traditional contrast estimates. Intriguingly, the face motor cortex and the cerebellum, typically associated with speech production, and the orbitofrontal cortex, linked to visual recognition and working memory, additionally emerged as densely connected components of the network. The left inferior occipitotemporal cortex, involved in early letter-string or word-specific processing, and the cerebellum turned out to be the main forward driving nodes of the network. Synchronization within a subset of nodes formed by the left occipitotemporal, the left superior temporal, and orbitofrontal cortex was increased with the subjects' effort to comprehend the text. Our results link long-range neural synchronization and directionality with cognitive performance.

Keywords: causality, coherence, connectivity, language, magnetoencephalography, synchronization

Introduction

Neuroimaging studies of language processing, and of human brain function in general, typically use so-called activation paradigms. In these experiments, different types of stimuli are presented to the subject, or s/he performs different tasks on the same set of stimuli, and the brain areas that show stronger signal in the “activation” condition versus a selected “baseline/control” condition are identified. In language studies, the stimuli have most often been isolated items, such as words, nonwords, or pictured objects. These relatively simple stimuli facilitate straightforward design of contrasts between stimuli and tasks that are assumed to reveal brain areas involved in specific subcomponents of language processing, such as semantic or phonological analysis (e.g., Jobard and others 2003; Wydell and others 2003). So far, research has focused primarily on where in the brain the active areas are located and at what time they are active with respect to stimulus/task timing. Functional magnetic resonance imaging (fMRI) and positron emission tomography (PET), using hemodynamic measures, typically seek answers in terms of location (Price and others 1994; Pugh and others 1996; Cohen and others 2000), whereas electroencephalography (EEG) sets the emphasis essentially on timing (Nobre and McCarthy 1994;

Hagoort 2003). Magnetoencephalography (MEG) combines accurate timing with a good estimate of the spatial distribution of active brain areas (Salmelin and others 2000; Halgren and others 2002).

However, the “where” and “when” descriptions are likely to provide only a partial and potentially inaccurate view of the neural implementation of language function. Importantly, one essential aspect has been largely untouched, namely, how language information is processed within this (partly known) network. Based on intracranial recordings, spatially distributed components of cerebral networks are assumed to connect via synchronized neuronal firing (Singer 1999; Tallon-Baudry and others 2001). A number of studies have sought to estimate functional and/or effective connectivity between brain areas from PET/fMRI data (Büchel and Friston 1998; Mechelli and others 2002, 2005; Penny and others 2004). Although these studies provide useful information of potential interactions in the brain, there are limitations. First, modeling of interactions is based on predefined regions that are typically selected among areas revealed by contrasting levels of activation between experimental conditions. It is important to note that time courses may be highly correlated even when the overall activation does not exceed noise level. Furthermore, the same brain area may be equally active in both experimental and control tasks and, therefore, not evident in the resulting contrast map. Consequently, relevant components of the functionally connected network may not emerge in the contrast analysis and would thus not be considered in the connectivity analysis either. Second, hemodynamic techniques provide a slow and delayed signature of neural activity, thus rendering evaluation of synchrony and direction of information flow between brain areas problematic.

Time-sensitive neuroimaging techniques, EEG and MEG allow real-time tracking of neural activity and should thus be ideal tools for characterizing the temporal dynamics of functional networks. Here, development of appropriate analysis methods has been hindered by the complex relationship between the electromagnetic field outside of the head and the location of neural activity within the brain; in case of EEG, the situation is further complicated by the large changes of electric conductivity between the brain, skull, and scalp. In simple motor tasks, an electromyogram (EMG) recorded from the moving muscles may serve as an external reference signal for localization of the primary motor cortex (based on EMG-MEG coherence) that can then be used as a cortical reference area for identifying other components of the motor network (Gross and others 2001, 2002). When meaningful nonbrain reference signals are not available to seed the analysis, which is typically the case in cognitive tasks, coherence analysis has so far been limited to the

level of EEG electrodes or MEG sensors, without reference to the actual source areas in the brain (Gerloff and others 1998; Sarnthein and others 1998; Andres and others 1999; Miltner and others 1999; Rodriguez and others 1999; Gross and others 2004; Palva and others 2005).

Here, we characterize real-time neural connectivity during reading. We determine the network nodes directly from interactions among whole-head MEG data, without prior assumptions of specific areas or network structure, and estimate both synchronization and direction of information flow between the nodes. Thus, we directly assess the question of “how” distinct brain areas work together to support cognitive behavior. Our analysis method is based on a beamformer technique optimized for the frequency domain, Dynamic Imaging of Coherent Sources (DICS), that was originally adapted for analysis of the motor system, with EMG as reference signal (Gross and others 2001, 2002). Here, we have developed DICS to allow identification of initial reference areas in the brain and, further, entire networks without need for nonbrain reference signals.

As this dynamic connectivity analysis only relies on timing at the neuronal level, without need for external trigger signals, it facilitates the use of continuous, increasingly realistic tasks that the human brain is tuned for. It should thus be possible to explore the brain working in a specific continuous mode as opposed to responding to single jolts. In a continuous task, one may also expect a higher signal-to-noise ratio of connectivity estimates than for isolated stimuli presented at intervals of a few seconds.

In the present study, we analyzed network dynamics during rapid serial visual presentation (RSVP) of connected text. RSVP is a pseudorealistic paradigm that simulates natural reading but without need for making saccades. Two aspects of the RSVP task were manipulated. First, connected text was presented at different rates to parametrically change the demands on visual word recognition and sentence comprehensibility. Second, comprehensibility was also varied by presenting words in a scrambled order, thereby disrupting the discourse. The RSVP timing was derived from the subjects' individual psychometric functions. To allow linking the present study with the existing neuroimaging literature on reading a more traditional design with isolated words and nonwords was included as well.

Our specific questions were the following: Can we identify neuronal networks associated with reading? Does the same network support both continuous reading and processing of isolated words/nonwords? How do the network nodes compare with activated areas typically reported in neuroimaging studies of reading? Does the interaction occur at specific frequencies? Are there preferred directions of information flow? Are the network properties affected by the effort or ability to comprehend the text?

We found a left-hemisphere cerebro-cerebellar network that resonated at 8–13 Hz, independent of the rate at which the words were presented. The overall network structure was similar for connected text and isolated words. Many of the network nodes, determined entirely based on their connectivity pattern, were in general agreement with areas reported to be active during reading, as collected from the different imaging modalities. Additionally, a number of other areas emerged as strongly connected nodes such as the cerebellum (CB) that, together with the inferior occipitotemporal cortex (OT), was the main driving node of the network. Connection strengths

within specific subsets of this network were modulated by the subjects' ability to follow and comprehend the text.

Materials and Methods

Subjects and Paradigm

Nine healthy, native English-speaking subjects (4 males, 5 females, 21–45 years) participated in this study, which was approved by the local ethics committee.

Behavioral Tests

As a prelude to the MEG study, all subjects participated in a behavioral experiment. The stimuli consisted of 200 sentences, randomly chosen from a battery of 430 sentences. The sentences were composed of 12 high-frequency words with no overt punctuation. The sentences were presented centrally, one word at a time (visual angle 1–4°). The words were presented at different intervals (17–136 ms). Subjects were required to read a sentence, and then at the termination of the sentence a star replaced the final word, which was the cue to the subject to repeat out loud the sentence they had just seen. A sentence was judged as having been read correctly if the meaning of the sentence was maintained, and the subject did not miss out any critical words. The average number of sentences read correctly was then calculated for each interval. From this psychometric function, 3 presentation rates were chosen that corresponded to the floor and ceiling levels for reading accuracy, and half-way between the floor and ceiling levels. These individually selected presentation rates were used in the MEG experiment.

MEG Experiment

In the RSVP task, words forming a continuous story were presented at the 3 behaviorally determined rates, in separate 5-min blocks. The stimuli were selected randomly from a pool of 8 excerpts from “Anne of Green Gables” books by L. M. Montgomery. At the fastest rate (20–30 words per second), the subjects were not able to comprehend the story, whereas at the slowest rate (5–12 words per second) the story was easy to follow. The medium presentation rate (10–20 words per second) corresponded to approximately 50% reading accuracy. In another block, words were presented in a meaningless order at the slow rate. The subjects' vigilance was checked by informal questioning after the experiment. In addition, we included a more traditional paradigm where subjects were shown words and pronounceable nonwords (6–7 letters, 100 stimuli per category), presented in a randomized order for 300 ms every 3 s, for 10–11 min in total. About 10% of the words/nonwords were replaced by a question mark that prompted the subject to read out loud the previous stimulus. The order of tasks was randomized both within the RSVP set and between the RSVP and word/nonword task.

Brain activity was recorded with an Elekta-Neuromag VectorView MEG system (Helsinki, Finland), band-pass filtered at 0.03–200 Hz and digitized at 600 Hz. Anatomical MRI were obtained with a 3T General Electric Signa system (Milwaukee, USA).

Data Analysis

Ideally, one would like to evaluate connectivity between all voxel pairs in the brain and test them for significance but currently this is not feasible within a reasonable amount of time. Therefore, a critical step in network analysis is to first identify some nodes of the network and use them as initial reference areas to find other nodes. In some cases, it is enough to identify a single nodal point to be used as a cortical reference. Here, the analysis proceeded as follows: 1) In each subject and for all experimental conditions, correlation of time courses of activation was calculated for all voxel pairs, for computational feasibility in a part of the brain (left-hemisphere cortex). 2) Voxels with the highest number of connections to other voxels were taken as initial reference areas. 3) Starting from these areas, network nodes were searched in the entire brain. This step should reveal additional, less densely connected nodes of the network, or nodes that are located outside the initial limited search area. 4) Networks identified in the individual subjects were compared to determine systematic group-level nodes. 5) Connectivity

between the time courses of activation in these node areas, transferred back to the individual brains, was quantified by estimating phase synchronization and Granger causality, and tested for significance. A detailed description of the analysis procedures is given below.

Correlation and Coherence

Correlation is a measure of similarity between amplitudes of 2 time series. Cross-correlation further includes information on systematic time shifts between the 2 time series. Cross-correlation has been commonly used to characterize correlation when the time series are locked to timed events. In continuous tasks, as in the present study, the analysis of similarity is often done in frequency space. Cross-spectral density can be calculated by multiplying the Fourier transformed signals of the time series. Coherence is obtained by normalizing the cross-spectral density with the power spectral density of both time series. Its value ranges from 0 (no similarity) to 1 (identical time series).

Selection of Frequency Range

An essential step in correlation analysis is to select the frequency ranges of interest. The passbands relevant for long-range synchronization during reading were estimated at the sensor level. This was done by counting, for each MEG sensor, the number of other sensors with which it showed significant coherence. The 99% confidence level was estimated from surrogate data. Surrogate data were created by shuffling the time points of the original data, while preserving the spatial relationships (Halliday and others 1995; Gross and others 2001). To focus on long-range coherence, the 2 nearest sensors in each direction were excluded in this calculation.

Coherence Imaging

DICS (Gross and others 2001) can be used to estimate both activity in different voxels and real-time long-range connectivity between brain areas directly from MEG data. DICS is a beamforming technique (Sekihara and Scholz 1996; Robinson and Vrba 1997; Van Veen and others 1997; Gross and Ioannides 1999), that is, it uses a spatial filter to maximize the signal from one voxel while suppressing activity from other voxels. In DICS, the time series recorded by the MEG sensors are transformed into frequency domain by computing cross-correlation spectra for all sensor combinations. The resulting cross-spectral density matrix ($m \times m \times f$; m = number of MEG sensors, f = number of frequency bins) represents the oscillatory components and their linear interactions. As cross-correlation spectra retain the signal strength and phase (timing) relationships among the sensor sites, the brain areas generating the signals can be localized. Here, the cross-spectral density was computed using Welch's method of spectral density estimation (Welch 1967; Gross and others 2001). DICS was used to image coherence in the brain at a given frequency range, thresholded, and overlaid on individual anatomical MRIs. The 99% confidence level was estimated from surrogate data (see above, Selection of frequency range). For additional information, see Supplementary Text S1, Figure S1.

Reference Area Localization

The initial search for reference areas was performed by computing connection density estimates (CDEs). CDEs were formed by counting, for each voxel, the number of connections to other voxels for which coherence exceeded a chosen threshold. To emphasize long-range connections and to minimize spatial blurring, the immediate neighborhood of each voxel was excluded (distance between coherent voxels at least 3.5 cm). The results are presented as normalized density statistical parametric maps (dSPM), overlaid on anatomical MRIs (Dale and others 2000). These maps depict the relative level of connectivity of all cortical areas during the task. The CDEs were obtained by dividing the left-hemisphere cortex into voxels of 6-mm side length and by using DICS to compute coherence between all voxel combinations. Connection density estimation was performed in one hemisphere to minimize spurious results. In beamformer methods, occurrence of low signal-to-noise ratio (SNR) (therefore, low spatial resolution) in some areas and symmetrical conductor geometry may result in artifactual effects. In the case of DICS, such artifacts could show as spurious coherence, for example, between areas symmetrically

positioned in the 2 hemispheres if the whole brain was included in the CDE computation. Focal maxima from the CDE maps were taken as initial reference areas. The analysis was done separately for each subject to maximize the localization accuracy of the reference areas (see Supplementary Text S2, Fig. S2).

Network Localization

Thereafter, coherence was calculated between these reference areas and the entire brain (divided into voxels of 6-mm side length), separately for each subject and each experimental condition. Depending on the strength of coherence and separability of areas, 1–4 connections were found per reference area and per condition. DICS analysis can reliably separate areas that are located at least 2 cm from each other; the accuracy of localization is typically a few millimeters, depending on the SNR in the imaged area (Liljeström and others 2005). The resulting areas across conditions were brought together and cluster centers were identified as individual nodal points.

The coherence values between all these nodal points were tested for significance (99% confidence level, surrogate data), separately for each subject. The resulting sets of significant nodal points from all subjects were transferred to a common coordinate system using an elastic transformation (Schormann and Zilles 1998). The individual nodes were given a spatial extent twice the voxel size used in the search for connected areas to account for the spatial sampling resolution and individual variability in the functional location of the regions. The data were composed of 1s and 0s; 1 indicated that there was at least one significant connection to/from the area, and 0 that there was none. The SPM2 software (Wellcome Department of Imaging Neuroscience, University College London, United Kingdom, <http://www.fil.ion.ucl.ac.uk/spm/spm2.html>) was used to test whether the significantly connected areas identified at the individual level appeared systematically across subjects. Areas passing this intersubject consistency test (minimum of 4 subjects) were taken as group-level nodal points of the network.

To further characterize the network properties (phase synchrony, direction of information flow), these group-level nodes were transferred back to the individual brains (Schormann and Zilles 1998). If any of group-level nodes transferred to a subject's brain fell within 1 cm of the network nodes initially determined for that subject, the individual nodal points were used instead of the group-level nodes. This was done to maximize the SNR in quantification of connectivity; 4–7 subjects had an individual node within 1 cm of a group-level node.

Talairach Coordinates and Labels

The nodal points of each subject were transferred to MNI coordinates using SPM2. The corresponding Talairach coordinates were determined using a nonlinear transform of MNI to Talairach (Brett and others 2002). Talairach labels were obtained using the Talairach Daemon (Lancaster and others 1997), separately for each subject. The Talairach coordinate reported is the average of the Talairach coordinates of the individual nodal points.

Phase Synchronization

Similarity of signal phase is frequently thought to be a more relevant measure of neural synchrony than cross-correlation or coherence that are also influenced by the possible interaction of the amplitude changes in the signals (Varela and others 2001). The time courses of activation at the nodal points were extracted with DICS (Gross and others 2001). The phase synchronization index (SI) (Tass and others 1998) between each pair of nodal points was calculated by applying the Hilbert transform on 1-s time windows (3-Hz band) and averaging across the entire recording. The 99% confidence levels for the SI values were estimated by randomly shuffling the time points 1000 times. The significance of task effects at the group level was evaluated using nonparametric Kendall's τ test ($P < 0.05$), and pairwise comparison was done with the Wilcoxon signed-ranks test ($P < 0.05$).

Direction of Information Flow

It is also possible to evaluate whether activity in one cortical area drives neural populations in another area. Here, the direction of information flow between nodal points was calculated using a method also applied to fMRI connectivity analysis (Roebroeck and others 2005) that is based on

Granger causality (Granger 1980). This calculation was performed directly on the time series of the nodal points (as opposed to phase coupling estimated with SI). Multivariate autoregressive models were used to estimate the direction of causality between 2 nodal points, conditional on all other nodal points. This controls for spurious causality that may occur because of the influence of a third area (e.g., common input). A 10th order model was chosen, based on the level of complexity of the MEG time series, using various order selection criteria (Roebroeck and others 2005). The amount of time during which the causality exceeded an estimated critical value (at $\alpha = 0.05$) was calculated between all areas, for both directions. Wilcoxon signed-ranks test ($P < 0.05$) was used to determine the dominant direction of causality at the group level, separately for each task.

Results

Behavioral Data

The psychometric function of reading accuracy by presentation rate (Fig. 1*A,B*) was determined prior to the MEG recording and used for setting the stimulus timing, individually for each of the 9 subjects. Figure 1*A* illustrates this procedure for one subject. At the slow rate (9 Hz), the text was easy to follow. At the fast rate (30 Hz), the subject was able to read the words but not comprehend the story. The medium rate (20 Hz) was set to half-way between the floor and ceiling level.

Figure 1*B* depicts the average psychometric function (mean \pm standard deviation [SD]) across subjects. The curves were similar in shape but showed large interindividual variability along the frequency axis. The slow rate varied from 5 to 12 Hz (mean 8 Hz), medium rate from 10 to 20 Hz (mean 15 Hz), and fast rate from 20 to 30 Hz (mean 25 Hz). By selecting the stimulus presentation rates separately for each subject on the

basis of her/his psychometric function we sought to equate the cognitive performance across subjects as well as possible.

Frequency Range of Interest

Figure 1*C* illustrates, for one subject (cf. Fig. 1*A*), a salient maximum in the sensor-level coherence spectrum at about 11 Hz. Task effects were also detected at this same frequency, as evidenced by the modulation of the peak level by reading condition. A maximum at 8–13 Hz, with the level influenced by task, was the most consistent finding also at the group level (8/9 subjects, Fig. 1*D*); 4 subjects had an additional maximum at 16–24 Hz. A similar pattern was evident on all sensors. In the subsequent analysis, we focus on the 8–13 Hz range.

The MEG sensors with the highest number of connections to other sensors at the frequency range of 8–13 Hz were typically located over the temporal and frontal areas (Fig. 2*A*). In contrast, the maximum power at 8–13 Hz (Fig. 2*B*) was concentrated to sensors over the parietal and occipital cortex and medially over the central sulcus. Accordingly, the spatial distribution of coherence in the 8–13 Hz range was not simply accounted for by a high level of rhythmic activity in those areas.

Networks in Individual Subjects

Figure 3*A* displays the 8–13 Hz CDE maps for RSVP (medium rate) and isolated word/nonword reading in the same subject for whom sensor-level data were depicted in Figure 2*A* (for data of the other subjects, see Supplementary Text S3, Fig. S3). The most densely connected voxels were concentrated to inferior frontal, temporal, and occipital areas. The distribution was remarkably similar for all experimental conditions; this was the case for all subjects. From these individual CDE maps it was

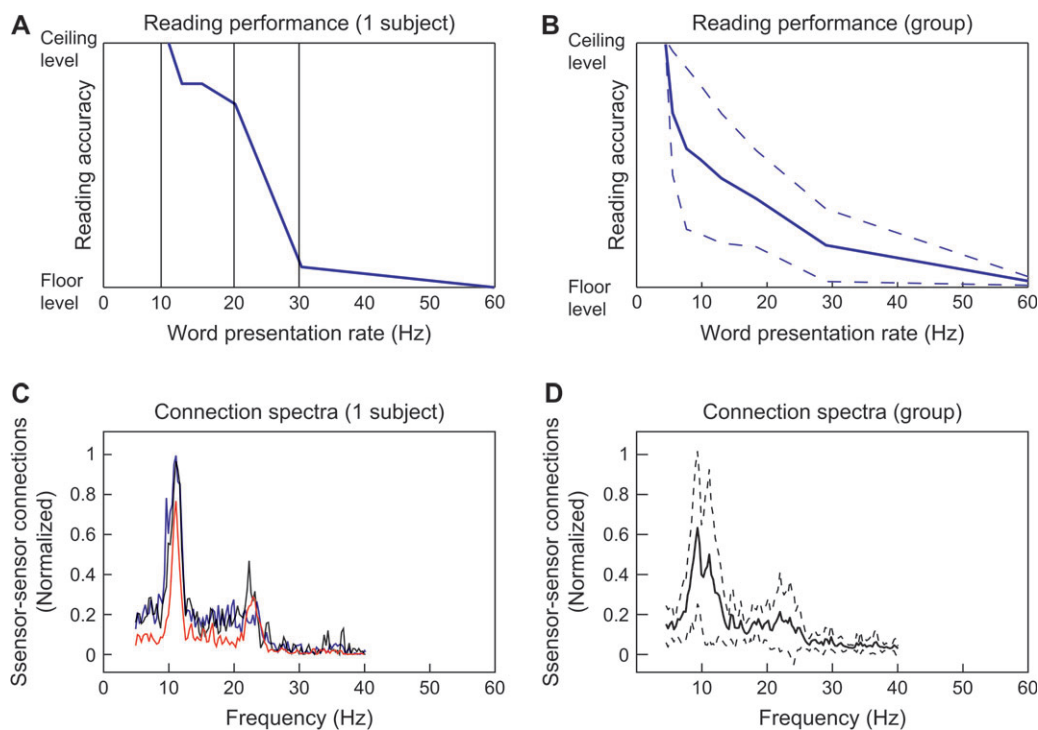


Figure 1. Behavioral and brain frequencies in reading. (A) Reading accuracy in one subject as a function of word presentation rate in the behavioral test. The vertical lines indicate the 3 rates representing the floor and ceiling level, and approximately half-way between those levels. (B) Reading accuracy versus presentation rate in all 9 subjects (mean \pm SD). (C) Coherence spectra for a selected MEG sensor, in the subject depicted in (A). The number of coherent sensor-sensor connections is plotted as a function of frequency. Presentation of the story at the fast (red), medium (black), and slow rate (blue). (D) Coherence spectra in all 9 subjects (mean \pm SD), plotted for the medium presentation rate. The spectra were normalized to the maximum number of connections in each subject.

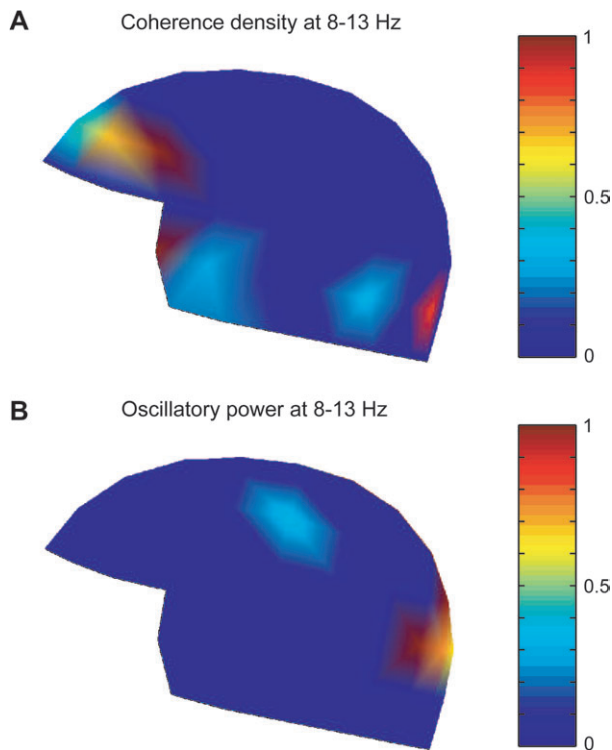


Figure 2. Distributions of coherence and power at sensor level. Example from one subject. (A) Spatial distribution of the number of coherent sensor-sensor connections in the 8–13 Hz range, at the medium presentation rate, displayed on the MEG helmet. The map was normalized to the highest number of connections per sensor. (B) Spatial distribution of normalized oscillatory power in the 8–13 Hz range, at the medium presentation rate. The planar gradiometers of the MEG system used in this study detect the maximum signal directly above an active brain area.

possible to identify 4–8 focal maxima per condition. The center points of the maxima in the different experimental conditions were pooled together, resulting in 7–11 distinguishable reference regions per subject.

Using these nodes as reference areas to search for connections in the entire brain revealed 3–11 additional connected areas per subject. All possible pairs of this total set of nodal points were tested for significant coherence (see Materials and Methods), resulting in a final set of 12–18 significantly connected nodes per subject. Figure 3(B) illustrates the significant network nodes for the subject depicted in Figure 3(A), including RSVP (medium rate) and isolated word/nonword conditions, and the final set compiled from all conditions. In the medium-rate RSVP condition 10 areas were significantly coherent (15 connections), and in the isolated word/nonword condition 8 areas (10 connections). The nodes identified for isolated word/nonword reading formed a subset of those detected in the RSVP condition. In this subject, the final set was composed of altogether 12 significantly coherent nodes, forming 17 connections (for the final set of nodes in the other subjects, see Supplementary Text S4, Fig. S4).

No additional areas were uncovered when network analysis was performed in the 16–24 Hz range. Using the stimulus presentation rate as the frequency of interest did not yield consistent nodal points beyond the occipital visual cortex. When the initial search for reference areas was performed in the right hemisphere, followed by mapping of coherence in the entire brain, no systematic network structures emerged (see Supplementary Text S5, Fig. S5).

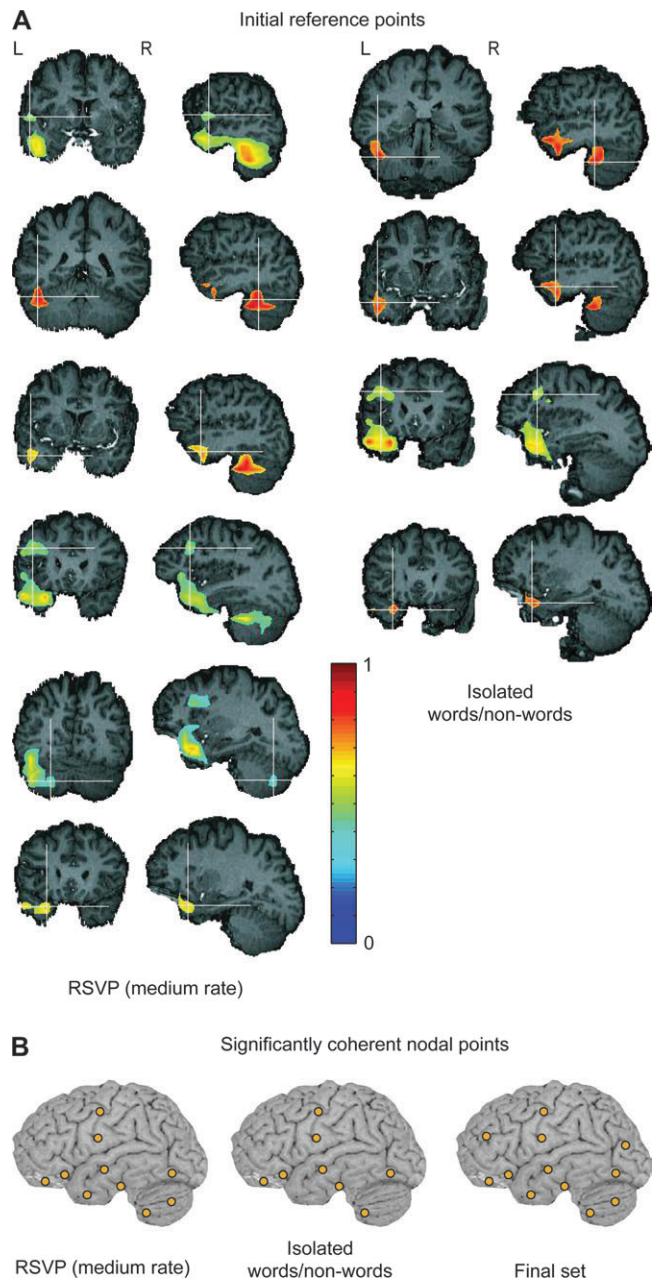


Figure 3. Network in a single subject. (A) Initial reference points for the subject depicted in Figure 2. Focal maxima of connection density maps (CDEs) at 8–13 Hz in the left-hemisphere cortex for the medium-rate RSVP task (left) and isolated word/nonword condition (right). The slices advance from lateral (top) to medial (bottom) areas. The CDE maps were normalized to the highest number of connections per voxel. (B) Significantly coherent nodal points in the left hemisphere for the medium-rate RSVP and isolated word/nonword conditions, and the final set of nodal points compiled from all conditions.

Group-Level Findings

Across subjects, the nodal points showing significant coherence with other brain areas were concentrated to the left hemisphere (Fig. 4), with only scattered, nonconsistent foci in the right hemisphere. By transferring the individual nodes into a common coordinate system we identified 9 distinct areas: inferior OT (approximately corresponding to Brodmann area [BA] 37; Talairach coordinates $-36, -59, -1$), medial temporal cortex (MT; BA 20; $-36, -39, -15$), superior temporal cortex (ST; BA 22; $-52, -6, -3$), anterior part of the inferior temporal cortex

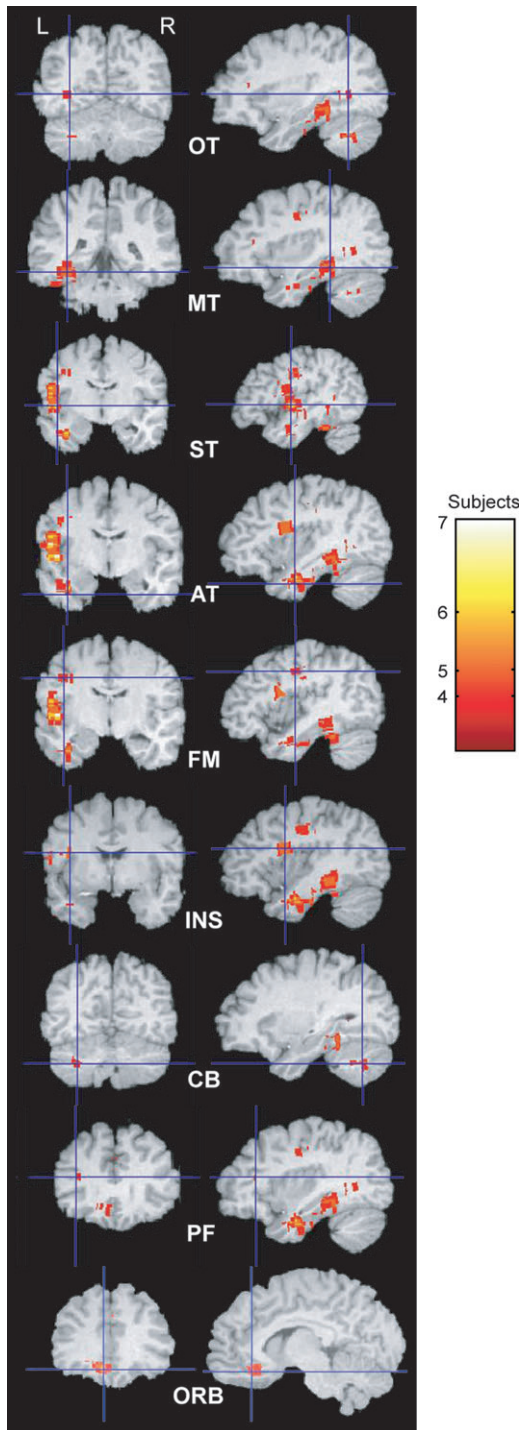


Figure 4. Group-level nodal points of neural connectivity. Section overlays of brain areas in which the time courses of activation at 8–13 Hz were significantly coherent with those in other regions of the brain. This map represents intersubject consistency of spatial location of the nodes (color indicates number of subject). OT = inferior occipitotemporal cortex, MT = medial temporal cortex, ST = superior temporal cortex, AT = anterior part of the inferior temporal cortex, FM = face motor cortex, INS = insula, CB = cerebellum, PF = prefrontal cortex, ORB = orbital cortex.

(AT; BA 21; $-34, -4, -34$), precentral cortex about 15 mm below the hand knob, approaching the face motor cortex (FM; BA 4; $-46, -12, 37$), insula (INS; $-41, 1, 17$), CB ($-30, -61, -36$), prefrontal cortex (PF; BA 46; $-39, 29, 13$), and orbitofrontal cortex (ORB; BA 11; $-9, 34, 16$).

Characterization of Connectivity

Phase synchrony is frequently considered a more direct measure of neural interaction than linear coherence that mixes the effects of amplitude and phase. If phase locking is the relevant biological mechanism of brain integration, then a measure which is independent of amplitude should be suitable for describing cortico-cortical interactions in more detail (Varela and others 2001). Accordingly, we further computed the SI (Tass and others 1998), a nonlinear measure of phase coupling between 2 time series, to characterize the network dynamics between all these nodal points. For each connection in each individual subject, SI was calculated as a function of frequency, at 1-Hz intervals, and the peak value of the SI spectrum was taken as the level of phase coupling (Fig. 5A). The peak frequencies varied from 8 to 12 Hz, with no significant differences between the experimental conditions (mean values 8.9–9.2 Hz).

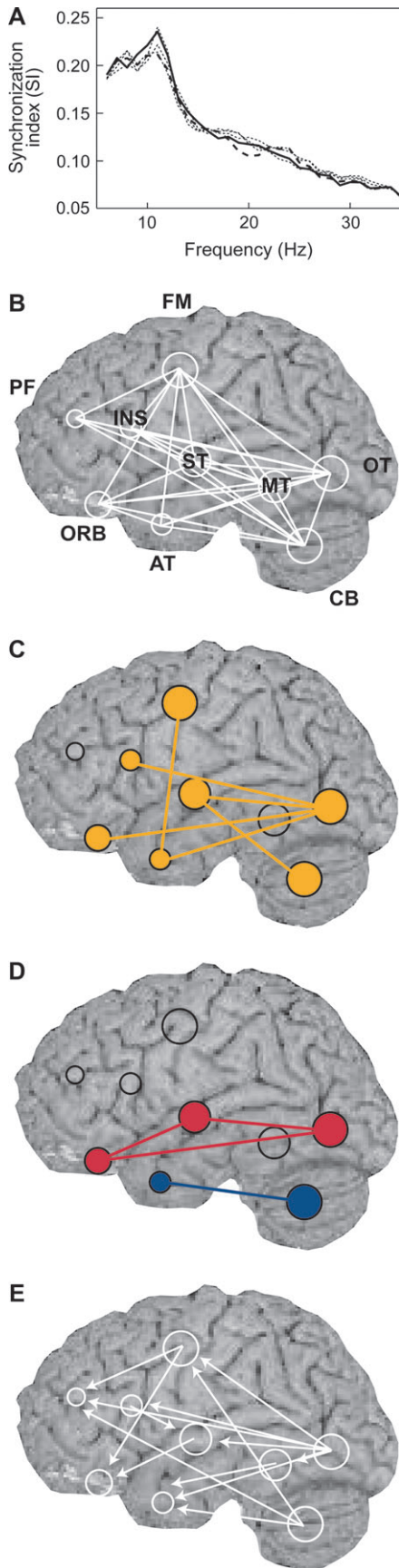
Figure 5(B) depicts overall connectivity between the nodal points, that is, connections for which SI was significant in at least 8 of the 9 subjects in one or more RSVP experimental conditions (mean SI 0.22–0.24 across subjects). OT, FM, and CB were the most densely connected regions (with all the other areas), and PF the most sparsely connected region (with 4 other areas). Each area was connected, on average, to 6 other areas.

These connections were further tested for significant task effects. The presentation rate in the RSVP task was at least 10 times that for the isolated words/nonwords. The result was, in particular, stronger synchronization (mean 9.4%) of the posterior OT area with the frontal ORB area and temporal areas ST/AT (Fig. 5C). Within the RSVP tasks, faster presentation rate of a story further enhanced synchronization (5.3%) within a subset of these connections, in a network formed by ORB, ST, and OT (Fig. 5D). From slow to fast reading condition, synchronization between OT and ST increased in every subject. Presentation of meaningful versus scrambled text showed remarkably similar patterns of connectivity. The only difference (Fig. 5D) was stronger synchronization (3.6%) in the meaningful than scrambled condition between CB and AT.

Coherence and phase synchrony are inherently non-directional measures. Therefore, we estimated the direction of information flow by Granger causality (Roebroeck and others 2005) (Fig. 5E) for the significant connections depicted in Figure 5(B). This analysis suggested directed interactions from the posterior to anterior areas during the RSVP tasks, with OT and CB as the main driving nodes. As for the precentral nodes, the information flow was predominantly from FM to PF and ORB, and from INS to the temporal lobe (ST). The remaining connections (cf. Fig. 5B) showed no dominant direction of information flow.

Discussion

MEG data were recorded while subjects were silently reading connected text (rate 5–30 Hz) or isolated words (rate 0.3 Hz). The RSVP technique is ideal for manipulating reading speed. It also minimizes the involvement of those cortical circuits normally contributing to the planning and execution of eye movements when a body of text is navigated. As a result, our analyses could be better focused on elucidating networks engaged in visual word recognition as well as sentence comprehension. MEG experiments which deal with the added complexity of eye-movement control will be an area for future study.



Voxel-based coherence analysis of the time courses of neural activity revealed a left-hemisphere network of densely interconnected areas. The spatial distribution of the network was similar for the pseudorealistic task of reading a continuous story at various behaviorally determined rates or a scrambled sequence of words, and for processing isolated stimuli.

Coupling was strongest at the frequency range 8–13 Hz, systematically across subjects, as indicated by both linear coherence and nonlinear synchronization measures. The consistency of the carrier frequency across subjects and experimental conditions was all the more remarkable as the stimulus rates, determined from the individual psychometric functions, varied along a wide range of frequencies. In about half of the subjects, a second, weaker maximum at 16–24 Hz appeared in the coherence spectra; its frequency was not affected by the stimulus rate, either. The network was thus most consistently resonating at the so-called alpha frequency (Berger 1929). The spatial distribution of the spectral power in this frequency range agreed with the known generator areas of the visual alpha rhythm in the occipital cortex and the parieto-occipital sulcus, and of the 10-Hz component of the somatosensory/motor mu rhythm in and around the hand representation area along the central sulcus (Hari and Salmelin 1997). The network involved in reading did not coincide with these areas of high alpha power. The alpha range may, nevertheless, be a natural frequency to use for efficient interareal transfer of information throughout the brain. Thalamic cells burst spontaneously at a frequency of about 10 Hz (Steriade and others 1990), and may well tune the construction of neural networks in the developing brain for optimal signal transfer in this particular frequency range. Cognitive functions and even consciousness have been suggested to be supported by neural synchronization at specific frequencies, most notably the gamma band (30–100 Hz; Singer 1999; Tallon-Baudry and others 2001), but also the alpha range (Klimesch and others 2005). Gamma synchronization probably occurs relatively locally, whereas long-range synchronization relies on lower-frequency oscillations (Kopell and others 2000), in line with the present data.

Several of the nodes determined with the present “how” analysis are in general agreement with areas found in activation studies focusing on “where” and “when” in single-word reading. The left inferior OT is likely to be involved in early transition from visual to linguistic analysis. Neurophysiological studies (intracranial recordings, EEG, MEG) have associated activation of this area in reading tasks with letter-string specific analysis (Nobre and others 1994; Tarkiainen and others 1999) and hemodynamic studies (PET, fMRI) more specifically with word

Figure 5. Connectivity within the network and task effects. (A) SI as a function of frequency between the time courses in OT and ORB for all 5 conditions, in one subject. Fast RSVP task shown with solid line (strongest SI), isolated words/nonwords condition with dashed line (weakest), and medium, slow, and scrambled conditions with thin dotted lines (in between). (B) Overall connectivity between the nodal points (SI exceeded 99% confidence level for 8 out of 9 subjects at least in one RSVP condition). The size of the nodal point indicates how many other points it was connected with. (C) Connections for which SI was significantly higher in at least one RSVP condition than when reading isolated words/nonwords. (D) Connections for which the SI in the RSVP tasks differed from each other. Red indicates significant effect of presentation rate on the SI (fast/medium > slow) and blue the effect of story coherence at the slow rate (meaningful > scrambled). (E) Direction of information transfer (arrows), estimated using Granger causality, and pooled over the RSVP conditions. Whenever significant ($P < 0.05$) causality between 2 nodal points was detected, it was always in the same direction.

form analysis (Cohen and others 2000; McCandliss and others 2003). Activation of the left ST is a salient and consistent finding in MEG studies of reading, reported to reflect semantic (Helenius and others 1998; Halgren and others 2002), but also phonological, analysis (Wydell and others 2003). Hemodynamic studies, however, tend to associate ST activation primarily with phonological processing (Jobard and others 2003). The medial (MT) and anterior temporal lobe (AT) are likely to play a role specifically in comprehension, as suggested by intracranial recordings (Nobre and others 1994; McCarthy and others 1995) and hemodynamic studies (Rossell and others 2003). Some MEG data have also implied activation of these areas in reading (Halgren and others 2002).

Our connectivity analysis thus revealed a set of areas that show considerable overlap with those reported in fMRI, PET, MEG, and/or intracranial activation studies. Interestingly, however, the observed network did not include the supramarginal gyrus or posterior ST that are thought to be involved in grapheme-to-phoneme conversion (Jobard and others 2003). In part this may be because rapid, skilled reading probably relies more heavily on lexical-semantic than analytic, phonological analysis. It is also possible that these areas exert a slowly varying modulatory influence rather than participate in the rapid signal transfer within the network and would, therefore, not manifest themselves in the coherence analysis.

The network also included nodes that have been associated primarily with language production rather than perception in activation studies. The general region of the left inferior frontal cortex has been suggested to be involved in multiple aspects of language perception, ranging from phonology and semantics to analysis of syntax (Dapretto and Bookheimer 1999; Jobard and others 2003). In the present network analysis, however, the node was centered on the INS, which has been related more specifically to speech production (Dronkers 1996; Wise and others 1999). Furthermore, the network included the FM and the CB that are typically active in speech production (Wildgruber and others 2001) and vocalized reading (Fiez and Petersen 1998).

Moreover, the network encompassed the ORB and the left PF that have not been reported specifically in reading tasks but, rather, in experiments focusing on visual recognition and working memory (Petrides and others 2002; Rolls 2004). The ORB is directly connected to the inferior, anterior, and superior temporal cortex (Rolls 2004), the “what” stream of visual analysis (Ungerleider and Haxby 1994).

The inferior OT, the FM, and the CB were connected to all other nodes. The dense coupling of the OT seems reasonable because of its proposed role at the interface between visual and linguistic analysis in reading. The FM and CB, however, are less obvious choices as major nodes in silent reading (but see Price and others 1994). The CB has been suggested to play a role in event timing, also in perception (Ivry 1996), the former being a potentially important issue in the present paradigm. Alternatively, the dense coupling of both FM and CB in the network may point to actual involvement of the motor system in silent reading. When learning to read children typically need to speak the words out loud. As adults, we usually need to make no mouth movements to process written language and, in the present RSVP task, there was no time for that either. Nevertheless, our findings point to the possibility that speech production may be intricately interwoven with the process of reading. Brought to an extreme, one may ask

whether a “motor theory of reading,” akin to the “motor theory of speech perception” connecting auditory and gestural features (Lieberman and Mattingly 1985; for neuroimaging evidence see, e.g., Hickok and Poeppel 2004; Wilson and others 2004; Vigneau and others 2006), should be considered for visual language perception as well.

For the most part, the connections were bidirectional (feedforward and feedback), as the Granger causality estimates did not reveal a dominant direction. However, the importance of the OT as the main entrance point from visual analysis to the language network was emphasized by the dominant feedforward direction of information flow from this area to the other nodes. This finding makes it all the more understandable that functional underdevelopment of the left OT area, consistently reported in dyslexic individuals, may indeed severely impair the normal reading process (Salmelin and others 1996; Paulesu and others 2001). The CB emerged as the other main driving node of the network, most probably reflecting accurate tracking of the stimulus timing in the RSVP task (Ivry 1996). Both of these areas sent information to the FM, which in turn influenced activity in the ORB and PF involved in visual recognition. Indeed, one may ask whether the node associated here with FM could actually reflect involvement of the frontal eye field. However, this node was centered about 1 cm posterior, inferior, and lateral to the area functionally identified as the human frontal eye field (Nobre and others 1997).

The level of synchronization between specific nodal points varied with cognitive performance. The connections from the main driving nodes, OT and CB, were the ones most strongly affected by stimulation rate and comprehensibility. The 10-fold increase in stimulation rate from isolated words to RSVP tasks particularly enhanced synchronization from the word/letter area OT to AT and ST and to inferior and basal frontal cortex (INS, ORB), areas involved in linguistic and visual analysis.

When the presentation rate of a story within the RSVP task was increased synchronization was further enhanced within a concise network formed by the letter/word area OT, ST involved in semantic and phonological analysis, and the ORB area playing a role in visual recognition. The stronger synchronization suggests increasing pressure on the visual and semantic system for extracting the story line. However, when the presentation rate remained the same but the words did not form a meaningful sequence, synchronization was reduced between another set of areas, namely the temporal pole (AT) and the CB. Interestingly, an fMRI study using semantically related or unrelated word pairs reported modulation in these 2 areas, with temporal pole sensitive to semantic relatedness and cerebellum to the interval between the words (Rossell and others 2003). Interplay between these areas may thus be emphasized in processing a semantically meaningful sequence of words presented in a rapid succession. Whatever its precise role in reading, our data suggest that the cerebellum is intimately involved in complex cognitive tasks.

Accordingly, with an approach that is entirely data driven and independent from typical “activation paradigms” we detected an extensive left-hemisphere network during a continuous reading task, the nodal points of which partly matched the previously reported spatial distribution of active areas in single-word reading. We further determined nonlinear phase coupling and directionality within that network. This type of analysis is directly applicable to other cognitive questions in which no external, nonbrain reference signal is available.

An obvious question is whether the functional network of reading, determined directly from MEG data without prior assumptions of specific areas involved, matches anatomical connectivity in these individuals, as determined from diffusion tensor imaging (DTI) of white matter tracts (Mori and Van Zijl 2002). The nodes of the functional network should serve as excellent seed points for DTI analysis, which could again feed back to the functional analysis. For example, it will be of interest to study whether OT and FM might be connected directly or, perhaps, via the basal ganglia. If an additional junction were identified anatomically it would give strong impetus to further enhance the signal-to-noise ratio in the DICS analysis to improve detection of subcortical structures in natural reading.

Supplementary Material

Supplementary Material can be found at: <http://www.cercor.oxfordjournals.org/>.

Notes

We are grateful to Mika Seppä for help with coordinate transformations. This work was supported by the Finnish Ministry of Education, the James S. McDonnell Foundation 21st Century Research Award, the Academy of Finland Centre of Excellence Programmes 2000–2005 and 2006–2011, Sigrid Jusélius Foundation, The Wellcome Trust, the Lord Dowding Fund, and the European Union's Transnational Access to Research Infrastructures (Large-Scale Facility Neuro-BIRCH-III, operated at the Brain Research Unit, Low Temperature Laboratory, Helsinki University of Technology). *Conflict of interest*: None declared.

Address correspondence to Jan Kujala, Brain Research Unit, Low Temperature Laboratory, PO Box 2200, 02015 HUT, Finland. Email: jjkujala@neuro.hut.fi.

References

- Andres FG, Mima T, Schulman AE, Dichgans J, Hallett M, Gerloff C. 1999. Functional coupling of human cortical sensorimotor areas during bimanual skill acquisition. *Brain* 122:855–870.
- Berger H. 1929. Über das Elektroenkephalogramm des Menschen. *Arch Psychiatr Nervenkr* 87:527–570.
- Brett M, Johnsrude IS, Owen AM. 2002. The problem of functional localization in the human brain. *Nat Rev Neurosci* 3:243–249.
- Büchel C, Friston KJ. 1998. Dynamic changes in effective connectivity characterized by variable parameter regression and Kalman filtering. *Hum Brain Mapp* 6:403–408.
- Cohen L, Dehaene S, Naccache L, Lehericy S, Dehaene-Lambertz G, Henaff MA, Michel F. 2000. The visual word form area—spatial and temporal characterization of an initial stage of reading in normal subjects and posterior split-brain patients. *Brain* 123:291–307.
- Dale AM, Liu AK, Fischl BR, Buckner RL, Belliveau JW, Lewine JD, Halgren E. 2000. Dynamic statistical parametric mapping: combining fMRI and MEG for high-resolution imaging of cortical activity. *Neuron* 26:55–67.
- Dapretto M, Bookheimer SY. 1999. Form and content: dissociating syntax and semantics in sentence comprehension. *Neuron* 24:427–432.
- Dronkers NF. 1996. A new brain region for coordinating speech articulation. *Nature* 384:159–161.
- Fiez JA, Petersen SE. 1998. Neuroimaging studies of word reading. *Proc Natl Acad Sci USA* 95:914–921.
- Gerloff C, Richard J, Hadley J, Schulman AE, Honda M, Hallett M. 1998. Functional coupling and regional activation of human cortical motor areas during simple, internally paced and externally paced finger movements. *Brain* 121:1513–1531.
- Granger CWJ. 1980. Testing for causality: a personal viewpoint. *J Econ Dyn Control* 2:329–352.
- Gross J, Ioannides AA. 1999. Linear transformations of data space in MEG. *Phys Med Biol* 44:2081–2097.
- Gross J, Kujala J, Hämäläinen M, Timmermann L, Schnitzler A, Salmelin R. 2001. Dynamic imaging of coherent sources: studying neural interactions in the human brain. *Proc Natl Acad Sci USA* 98:694–699.
- Gross J, Schmitz F, Schnitzler I, Kessler K, Shapiro K, Hommel B, Schnitzler A. 2004. Modulation of long-range neural synchrony reflects temporal limitations of visual attention in humans. *Proc Natl Acad Sci USA* 101:13050–13055.
- Gross J, Timmermann J, Kujala J, Dirks M, Schmitz F, Salmelin R, Schnitzler A. 2002. The neural basis of intermittent motor control in humans. *Proc Natl Acad Sci USA* 99:2299–2302.
- Hagoort P. 2003. Interplay between syntax and semantics during sentence comprehension: ERP effects of combining syntactic and semantic violations. *J Cogn Neurosci* 15:883–899.
- Halgren E, Dhond RP, Christensen N, Van Petten C, Marinkovic K, Lewine JD, Dale AM. 2002. N400-like magnetoencephalography responses modulated by semantic context, word frequency, and lexical class in sentences. *Neuroimage* 17:1101–1116.
- Halliday DM, Rosenberg JR, Amjad AM, Breeze P, Conway BA, Farmer SF. 1995. A framework for the analysis of mixed time series/point process data—theory and application to the study of physiological tremor, single motor unit discharges and electromyograms. *Prog Biophys Mol Biol* 64:237–278.
- Hari R, Salmelin R. 1997. Human cortical oscillations: a neuromagnetic view through the skull. *Trends Neurosci* 20:44–49.
- Helenius P, Salmelin R, Service E, Connolly JF. 1998. Distinct time courses of word and sentence comprehension in the left temporal cortex. *Brain* 121:1133–1142.
- Hickok G, Poeppel D. 2004. Dorsal and ventral streams: a framework for understanding aspects of the functional anatomy of language. *Cognition* 92:67–99.
- Ivry RB. 1996. The representation of temporal information in perception and motor control. *Curr Opin Neurobiol* 6:851–857.
- Jobard G, Crivello F, Tzourio-Mazoyer N. 2003. Evaluation of the dual route theory of reading: a metaanalysis of 35 neuroimaging studies. *Neuroimage* 20:693–712.
- Klimesch W, Schack B, Sauseng P. 2005. The functional significance of theta and upper alpha oscillations. *Exp Psychol* 52:99–108.
- Kopell N, Ermentrout GB, Whittington MA, Traub RD. 2000. Gamma rhythms and beta rhythms have different synchronization properties. *Proc Natl Acad Sci USA* 97:1867–1872.
- Lancaster JL, Summerlin JL, Rainey L, Freitas CS, Fox PT. 1997. The Talairach Daemon, a database server for Talairach Atlas labels. *Neuroimage* 5:8633.
- Lieberman AM, Mattingly IG. 1985. The motor theory of speech perception revised. *Cognition* 21:1–36.
- Liljeström M, Kujala J, Jensen O, Salmelin R. 2005. Neuromagnetic localization of rhythmic activity in the human brain: a comparison of three methods. *Neuroimage* 25:734–745.
- McCandliss BD, Cohen L, Dehaene S. 2003. The visual word form area: expertise for reading in the fusiform gyrus. *Trends Cogn Sci* 7:293–299.
- McCarthy G, Nobre AC, Bentin S, Spencer DD. 1995. Language-related field potentials in the anterior-medial temporal lobe: I. Intracranial distribution and neural generators. *J Neurosci* 15:1080–1089.
- Mechelli A, Crinion JT, Long S, Friston KJ, Lambon Ralph MA, Patterson K, McClelland JL, Price CJ. 2005. Dissociating reading processes on the basis of neuronal interactions. *J Cogn Neurosci* 17:1753–1765.
- Mechelli A, Penny WD, Price CJ, Gitelman DR, Friston KJ. 2002. Effective connectivity and intersubject variability: using a multisubject network to test differences and commonalities. *Neuroimage* 17:1459–1469.
- Miltner WH, Braun C, Arnold M, Witte H, Taub E. 1999. Coherence of gamma-band EEG activity as a basis for associative learning. *Nature* 397:434–436.
- Mori S, Van Zijl PC. 2002. Fiber tracking: principles and strategies—a technical review. *NMR Biomed* 15:468–480.
- Nobre AC, Allison T, McCarthy G. 1994. Word recognition in the human inferior temporal lobe. *Nature* 372:260–263.
- Nobre AC, McCarthy G. 1994. Language-related ERPs: scalp distributions and modulation by word type and semantic priming. *J Cogn Neurosci* 6:233–255.

- Nobre AC, Sebestyen GN, Gitelman DR, Mesulam MM, Frackowiak RSJ, Frith CD. 1997. Functional localization of the system for visuospatial attention using positron emission tomography. *Brain* 120:515-533.
- Palva JM, Palva S, Kaila K. 2005. Phase synchrony among neuronal oscillations in the human cortex. *J Neurosci* 25:3962-3972.
- Paulesu E, Demonet JF, Fazio F, McCrory E, Chanoine V, Brunswick N, Cappa SF, Cossu G, Habib M, Frith CD, and others. 2001. Dyslexia: cultural diversity and biological unity. *Science* 291:2165-2167.
- Penny WD, Stephan KE, Mechelli A, Friston KJ. 2004. Modelling functional integration: a comparison of structural equation and dynamic causal models. *Neuroimage* 23(Suppl 1):S264-S274.
- Petrides M, Alivisatos B, Frey S. 2002. Differential activation of the human orbital, mid-ventrolateral, and mid-dorsolateral prefrontal cortex during the processing of visual stimuli. *Proc Natl Acad Sci USA* 99:5649-5654.
- Price CJ, Wise RJS, Watson JDG, Patterson K, Howard D, Frackowiak RSJ. 1994. Brain activity during reading. The effects of exposure duration and task. *Brain* 117:1255-1269.
- Pugh KR, Shaywitz BA, Shaywitz SE, Constable RT, Skudlarski P, Fulbright RK, Bronen RA, Shankweiler DP, Katz L, Fletcher JM, and others. 1996. Cerebral organization of component processes in reading. *Brain* 119:1221-1238.
- Robinson SE, Vrba J. 1997. Functional neuroimaging by Synthetic Aperture Magnetometry (SAM). In: Yoshimoto T, Kotani M, Kuriki S, Karibe H, Nakasato B, editors. Recent advances in biomagnetism. Sendai: Tohoku University Press. p 302-305.
- Rodriguez E, George N, Lachaux JP, Martinerie J, Renault B, Varela FJ. 1999. Perception's shadow: long-distance synchronization of human brain activity. *Nature* 397:430-433.
- Roebroeck A, Formisano E, Goebel R. 2005. Mapping directed influence over the brain using Granger causality and fMRI. *Neuroimage* 25:230-242.
- Rolls ET. 2004. The functions of the orbitofrontal cortex. *Brain Cogn* 55:11-29.
- Rossell SL, Price CJ, Nobre AC. 2003. The anatomy and time course of semantic priming investigated by fMRI and ERPs. *Neuropsychologia* 41:550-564.
- Salmelin R, Helenius P, Service E. 2000. Neurophysiology of fluent and impaired reading: a magnetoencephalographic approach. *J Clin Neurophysiol* 17:163-174.
- Salmelin R, Service E, Kiesilä P, Uutela K, Salonen O. 1996. Impaired visual word processing in dyslexia revealed with magnetoencephalography. *Ann Neurol* 40:157-162.
- Sarnthein J, Petsche H, Rappelsberger P, Shaw GL, von Stein A. 1998. Synchronization between prefrontal and posterior association cortex during human working memory. *Proc Natl Acad Sci USA* 95:7092-7096.
- Schormann T, Zilles K. 1998. Three-dimensional linear and nonlinear transformations: an integration of light microscopical and MRI data. *Hum Brain Mapp* 6:339-347.
- Sekihara K, Scholz B. 1996. Generalized Wiener estimation of three-dimensional current distribution from biomagnetic measurements. *IEEE Trans Biomed Eng* 43:281-291.
- Singer W. 1999. Neuronal synchrony: a versatile code for the definition of relations? *Neuron* 24:49-65.
- Steriade M, Gloor P, Llinás RR, Lopes da Silva FH, Mesulam M-M. 1990. Basic mechanisms of cerebral rhythmic activities. *Electroencephalogr Clin Neurophysiol* 76:481-508.
- Tallon-Baudry C, Bertrand O, Fischer C. 2001. Oscillatory synchrony between human extrastriate areas during visual short-term memory maintenance. *J Neurosci* 21:RC177.
- Tarkiainen A, Helenius P, Hansen PC, Cornelissen PL, Salmelin R. 1999. Dynamics of letter string perception in the human occipitotemporal cortex. *Brain* 122:2119-2132.
- Tass P, Rosenblum M, Weule J, Kurths J, Pikovsky A, Volkman J, Schnitzler A, Freund H-J. 1998. Detection of n:m phase locking from noisy data: application to magnetoencephalography. *Phys Rev Lett* 81:3291-3294.
- Ungerleider LG, Haxby JV. 1994. 'What' and 'where' in the human brain. *Curr Opin Neurobiol* 4:157-165.
- Van Veen BD, van Drongelen W, Yuchtman M, Suzuki A. 1997. Localization of brain electrical activity via linearly constrained minimum variance spatial filtering. *IEEE Trans Biomed Eng* 44:867-880.
- Varela F, Lachaux JP, Rodriguez E, Martinerie J. 2001. The brainweb: phase synchronization and large-scale integration. *Nat Rev Neurosci* 2:229-239.
- Vigneau M, Beaucousin V, Herve PY, Duffau H, Crivello F, Houde O, Mazoyer B, Tzourio-Mazoyer N. 2006. Meta-analyzing left hemisphere language areas: phonology, semantics, and sentence processing. *Neuroimage* 30:1414-1432.
- Welch P. 1967. The use of fast Fourier transform for the estimation of power spectra: a method based on time averaging over short, modified periodograms. *IEEE Trans Audio* 15:70-73.
- Wildgruber D, Ackermann H, Grodd W. 2001. Differential contributions of motor cortex, basal ganglia, and cerebellum to speech motor control: effects of syllable repetition rate evaluated by fMRI. *Neuroimage* 13:101-109.
- Wilson SM, Saygin AP, Sereno MI, Iacoboni M. 2004. Listening to speech activates motor areas involved in speech production. *Nat Neurosci* 7:701-702.
- Wise RJS, Greene J, Buchel C, Scott SK. 1999. Brain regions involved in articulation. *Lancet* 353:1057-1061.
- Wydell TN, Vuorinen T, Helenius P, Salmelin R. 2003. Neural correlates of letter-string length and lexicality during reading in a regular orthography. *J Cogn Neurosci* 15:1052-1062.